AD-A048 038 PENNSYLVANIA STATE UNIV UNIVERSITY PARK APPLIED RESE--ETC F/G 13/10
TURBULENCE LEVELS AND WAKE DIMENSIONS BEHIND A TOWED BODY.(U)
SEP 77 W R HALL, S HASSID N00017-73-C-1418
UNCLASSIFIED TM-77-260 NL

END
DATE FILMED
1-78
DDC

(12)

FC.

TURBULENCE LEVELS AND WAKE DIMENSIONS BEHIND A TOWED BODY

W. R. Hall and S. Hassid

Technical Memorandum
File No. TM 77-260
19 September 1977
Contract No. N00017-73-C-1418

Copy No. 14

The Pennsylvania State University
APPLIED RESEARCH LABORATORY
Post Office Box 30
State College, PA 16801

NAVY DEPARTMENT

NAVAL SEA SYSTEMS COMMAND

UNCLASSIFIED

SECURITY CLASSIFICATION OF THIS PAGE (When Data Entered)

REPORT DOCUMENTATION PAGE

READ INSTRUCTIONS BEFORE COMPLETING FORM

1. REPORT NUMBER: TM-77-260	2. GOVT ACCESSION NO.
3. RECIPIENT'S CATALOG NUMBER	
4. TITLE (and Subtitle): TURBULENCE LEVELS AND WAKE DIMENSIONS BEHIND A TOWED BODY.	5. TYPE OF REPORT & PERIOD COVERED: Technical Memorandum
	6. PERFORMING ORG. REPORT NUMBER
7. AUTHOR(s): W. R. Hall [redacted] S. Hassid	8. CONTRACT OR GRANT NUMBER(s): N00017-73-C-1418
9. PERFORMING ORGANIZATION NAME AND ADDRESS: Applied Research Laboratory, Post Office Box 30, State College, PA 16801	10. PROGRAM ELEMENT, PROJECT, TASK AREA & WORK UNIT NUMBERS: 24 p.
11. CONTROLLING OFFICE NAME AND ADDRESS: Naval Sea Systems Command, Washington, DC 20362	12. REPORT DATE: 19 Sep [redacted] 77
	13. NUMBER OF PAGES: 21
14. MONITORING AGENCY NAME & ADDRESS (if different from Controlling Office)	15. SECURITY CLASS. (of this report): UNCLASSIFIED
	15a. DECLASSIFICATION/DOWNGRADING SCHEDULE

16. DISTRIBUTION STATEMENT (of this Report)

Approved for public release. Distribution Unlimited.
Per NAVSEA - Nov. 25, 1977.

17. DISTRIBUTION STATEMENT (of the abstract entered in Block 20, if different from Report)

18. SUPPLEMENTARY NOTES

19. KEY WORDS (Continue on reverse side if necessary and identify by block number)

turbulence
wake
drag
lift
vortices
towed body
towing basin

20. ABSTRACT (Continue on reverse side if necessary and identify by block number)

Estimates of the turbulence intensity, its persistence and wake dimensions behind a towed body-of-revolution are presented. Contributors to this turbulence include the drag of the body and its towing strut as well as lift generated by the strut due to any misalignment with the tow direction and secondary vortices from the strut/sting intersection. Indications are that if turbulence resulting from body drag were the only consideration, the turbulence would decay to less than 0.10 percent within the time required to

DD FORM 1 JAN 73 1473 EDITION OF 1 NOV 65 IS OBSOLETE

UNCLASSIFIED

SECURITY CLASSIFICATION OF THIS PAGE (When Data Entered)

391 007

return the carriage to the starting point for another run. Calculations that include the drag of the strut show that the waiting time between test runs lengthens slightly. Consideration of disturbances arising from a one degree misalignment of the towing strut results in disturbances of the same order to magnitude as those arising from the drag of the body. Disturbances arising from the secondary vortices have been found to be negligible. An RMS total of all disturbances indicate that a 2-3 minute wait between test runs should be adequate to insure a turbulence level of less than 0.1 percent in the towing basin. ←

Subject: Turbulence Levels and Wake Dimensions Behind a Towed Body

References: See page 15.

Abstract: Estimates of the turbulence intensity, its persistence and wake dimensions behind a towed body-of-revolution are presented. Contributors to this turbulence include the drag of the body and its towing strut as well as lift generated by the strut due to any misalignment with the tow direction and secondary vortices from the strut/sting intersection. Indications are that if turbulence resulting from body drag were the only consideration, the turbulence would decay to less than 0.10 percent within the time required to return the carriage to the starting point for another run. Calculations that include the drag of the strut show that the waiting time between test runs lengthens slightly. Consideration of disturbances arising from a one degree misalignment of the towing strut results in disturbances of the same order of magnitude as those arising from the drag of the body. Disturbances arising from the secondary vortices have been found to be negligible. An RMS total of all disturbances indicate that a 2-3 minute wait between test runs should be adequate to insure a turbulence level of less than 0.1 percent in the towing basin.

Acknowledgment: This work was sponsored by the Naval Sea Systems Command, NAVSEA Code 0351.

Table of Contents

List of Tables

List of Figures

Nomenclature

A	$\pi/4\ d^2$, maximum body cross sectional area, ft^2
AR	b^2/S, strut aspect ratio
C_D	$D/1/2\rho V_o^2 A$, drag coefficient based on body cross sectional area
C_{D_s}	$D/1/2\rho V_o^2 S$, strut drag coefficient based on planform area
C_f	skin friction drag coefficient, Schoenherr friction factor
C_L	$L/1/2\rho V_o^2 S$, strut lift coefficient
C_ℓ	strut section lift coefficient, for an assumed elliptical distribution $C_L = C_\ell$
$C_\forall$	$\forall/A\ell$ body prismatic coefficient
D	drag, lbs
K, K_1, K_2	proportionality constants from experimental data
L	strut lift, lbs
Re_c	$V_o c/\nu$, Reynolds number based on strut chord
Re_ℓ	$V_o \ell/\nu$, Reynolds number based on body length
S	strut planform area, ft^2
V_o	free stream velocity, ft/sec
$\forall$	body volume, ft^3
$Z_{1/2}$	wake half-width or radius, ft
a	acceleration, ft/sec^2
b	tow strut span, also depth of submergence, ft
c	strut chord, ft
d	maximum body diameter, ft
g	acceleration due to gravity, 32.2 ft/sec^2
ℓ	overall body length, ft
t	time measured from origin, sta Ⓐ , seconds

t_o	local space time at a given station, time required for body to pass the station, seconds
th	maximum strut thickness, ft
$\sqrt{u^2}$	mean streamwise turbulence level, ft/sec
x	$V_o(t-t_o)$, distance behind the body, ft
y	independent length variable normal to body surface, ft
Γ_o	strut root circulation
α	strut angle-of-attack, degrees
δ	boundary layer displacement thickness, ft
ε	energy dissipation factor
θ	boundary layer momentum thickness, ft
λ	turbulence length scale, ft
ν	fluid kinematic viscosity, ft^2/sec
ρ	fluid density, $lb\ sec^2/ft^4$

Background and Summary

There has been much discussion on the relative merits of testing low-drag, laminar-flow bodies-of-revolution in ARL's 48-inch diameter water tunnel or in DTNSRDC's high-speed towing basin. Part of this discussion centers on the ambient turbulence levels of each facility, an intensity level of less than 0.1 percent being accepted as adequate for laminar flow work. Recent ARL measurements, Reference (a), indicate that this level can be reached in ARL's 48-inch diameter water tunnel with the installation of 1/4-inch cell honeycomb and if the tunnel speed is at least 35 ft/sec. Of course, turbulence levels in DTNSRDC's towing basin can be reduced to an acceptable level by allowing sufficient time for the turbulence to decay between tests. The question confronting testing in the DTNSRDC towing tank involves not only the turbulence levels, but its sources and persistence. How long must one wait between tests?

In both facilities, turbulence is generated by the drag of the test body and its support strut, as well as by the lift of the support strut arising from any misalignment with the flow direction, and by the secondary vortices formed at the strut/sting intersection as shown in Figure (1). In the water tunnel, additional turbulence is generated by the tunnel pump impeller, turning vanes, etc.

For the towing basin, indications are that if turbulence resulting from the body drag were the only consideration, the disturbances would decay to less than 0.1 percent within the time required to return the towing carriage to the starting point for another run. Calculations that include the drag of the support strut show that the waiting time between test runs lengthens slightly. Consideration of the disturbances arising from a one degree misalignment of the towing strut with the flow direction contributes disturbances of the same order of magnitude as those arising from the drag of the body. Disturbances due to the secondary vortex flow at the strut/sting intersection have been found to be negligible. An RMS total of all these disturbances indicate that a 2-3 minute wait between test runs should insure a turbulance level of less than 0.1 percent in the towing basin.

DTNSRDC's high-speed towing basin is 22-ft wide and 16-ft deep for a length of 1300 ft. The basin has an additional 1600 ft which is 8-ft deep and is connected to the 1300 ft section by a linear ramp roughly 10-ft long. For laminar flow bodies, testing is restricted to the 16-ft deep section to avoid any spurious wave drag. The high-speed towing carriage (Carriage No. 5) weighs approximately 100,000 lbs, is driven by 12 electric motors, and can achieve a maximum speed of 40 kts when towing a submerged body. The maximum acceleration/deceleration rate for this carriage is 0.15 g. Basin water temperatures are typically 60-70 deg F depending upon the season. Filter pumps, which normally circulate the basin water and could produce unwanted turbulence, are shut off during tests with the laminar-flow bodies. The towing strut arrangement for the laminar flow bodies is shown in Figure (1). The towing bridge and the model/strut combination can be raised and lowered by means of an overhead crane at the east end of the basin building. Hence the body must remain in the water for both the forward (data) and return passes of the towing carriage. A more complete descriptoin of DTNSRDC facility may be found in Reference (b).

In past tests, the towing carriage has been started from rest in the 8-ft deep section of the basin and carefully brought up to a speed of 3-5 kts. When the ramp to the 16-ft deep section was reached, the carriage was accelerated to the desired test speed. This procedure maximized the time available at the constant test speed. For the present calculations, we would like to consider as typical, the towing strategy shown in Figure (2). After the carriage has accelerated to a constant 50 ft/sec, it maintains this speed for 1000 ft. Then, the remaining 300 ft of the deep basin is used to stop the carriage. At a 50 ft/sec test speed, this distance falls within the allowable 0.15 g maximum acceleration/deceleration limit for the carriage mentioned earlier. As soon as the carriage has stopped, it begins to return to the starting point at a speed of 2.5 ft/sec. Turbulence will be generated on both the forward (data) and return passes of the carriage since the body cannot be raised out of the water. Turbulence levels will be considered at three stations as shown in Figure (2). The time in seconds for the body to pass these stations on both passes is shown in Figure (2). At 50 ft/sec the forward (data) pass and deceleration take 30 seconds, while the return pass of the carriage requires 520 seconds.

For the present calculations, Table (1) presents some characteristics for a typical laminar flow body. For comparison, the characteristics of a typical conventional body of the same length-to-diameter ratio are also given in Table (1).

Turbulence Due to Body and Strut Drag

From the experiments of Pao and Lin, Reference (c), and Chevray, Reference (d), the following correlations for the turbulence intensity and wake half-widths behind an axisymmetric body-of-revolution may be obtained

$$\frac{\sqrt{\overline{u^2}}}{V_o} = \frac{0.55}{\left(\frac{x}{DC_D^{1/2}}\right)^{2/3}} \qquad (1)$$

and

$$\frac{z_{1/2}}{DC_D^{1/2}} = 0.44 \left(\frac{x}{DC_D^{1/2}}\right)^{1/3} \qquad (2)$$

for an $x/DC_D^{1/2} > 10$. In these equations, x is the distance behind the body. By using a Galilean transformation $x = V_o(t-t_o)$ where t and t_o are the time from the origin and the time required for the body to reach a given station respectively, these equations can be transformed into functions of time. In Figure (2), t_o is written below the stations Ⓐ , Ⓑ , and Ⓒ for both the forward (data) and return passes of the towing carriage. Using Equation (1), it is possible to estimate the turbulence intenstiy levels behind a body-of-revolution for the typical carriage run described earlier. In order to simplify the calculations, it was assumed that:

a) the drag coefficient of the body remains constant for both the forward and return passes of the towing carriage. This assumption is not too restrictive. From Equation (1), it can be seen that if x/D is constant, then the turbulence intensity will vary as $C_D^{1/3}$, and that the ratio of the turbulence intensities for a constant x/D and varying drag coefficients will go as

$$\frac{\left(\frac{\sqrt{\overline{u^2}}}{V_o}\right)_2}{\left(\frac{\sqrt{\overline{u^2}}}{V_o}\right)_1} = \left(\frac{C_{D_2}}{C_{D_1}}\right)^{1/3} . \qquad (3)$$

Hence, the drag coefficient must increase by a factor of eight to double the intensity level. When one considers adding the turbulence intensities of the forward (data) and return passes of the carriage, a common normalization velocity must be used, this doubling of the turbulence levels for the carriage return pass would introduce less than a six (6) percent change in the overall turbulence level estimate. On the carriage return pass normal increases in the body due to changes in Reynolds number amount to less than 25 percent.

b) The carriage starts its return to the origin as soon as the carriage stops.

c) The influence of the forward (data) and return passes of the carriage on the overall turbulence intensity level is additive. A root-mean-square total is used and is given by

$$\left(\frac{\sqrt{\overline{u^2}}}{V_o}\right)_{Total} = \left\{\left(\frac{\sqrt{\overline{u^2}}}{V_o}\right)_{Forward} + \left(\frac{\sqrt{\overline{u^2}}}{V_o}\right)^2_{Return}\right\}^{1/2} . \qquad (4)$$

A root-mean-square total is also used in adding the turbulence levels from various sources, i.e., body drag, strut drag, strut lift, and secondary vorticity. Here it is assumed that the turbulence length scales are different between the various turbulence sources. For these calculations, and the ones following for other sources, the turbulence levels calculated will be centerline values. As such, they will be over-estimates of the general turbulence levels in the towing basin.

For a typical low-drag, laminar flow body described in Table (1), following the towing strategy outlined in Figure (2), Figure (3) presents the basin turbulence levels as a function of time from the start of the carriage forward (data) pass. The increases in turbulence level occurring at 150, 350 and 550 seconds at stations Ⓒ , Ⓑ and Ⓐ respectively, reflect the return pass of the carriage.

An estimate of the turbulence contributed by the drag of the towing strut of Figure (1) can be made by considering its turbulent skin friction drag and making an allowance for the cylindrical sting and stabilizing fins. At 50 ft/sec and with a chord of 5 ft, the strut Reynolds number is 2.25×10^7. Thus results in a Schoenherr skin friction coefficient of 0.002581 based on wetted surface area. The wetted surface area of the strut (2 sides) is 70 ft^2. Since one would like to use Equation (3) to scale the turbulence intensities for the strut rather than repeating all the individual calculations, the strut skin friction drag coefficient based on the maximum cross-sectional area of the laminar flow body is 0.085. Allowing an additional drag coefficient of 0.011 to account for the profile drag of the strut, the skin friction of the cylindrical sting and stabilizing fin drag, brings the total strut drag coefficient to 0.096 or eight times the drag coefficient of the laminar flow body. Using Equation (3) the turbulence intensity generated by the strut will be twice that of the laminar flow body. This result is plotted as Figure (4). A complete description of the towing strut is given in Table (1).

Figure (5) shows a plot of the turbulence intensity ratios using Equation (3) for various drag coefficient ratios. For example, the drag coefficient for the conventional body shape from Table (1) is five times that of the laminar flow body. Hence at the same distance behind the body (x/D = constant), the turbulence level generated by the conventional body will be 1.71 times that of the laminar flow body.

Turbulence Due to Strut Misalignment

Considering Figure (1), a slight misalignment between the towing strut and the tow direction appears entirely possible. Measuring from the rails upon which the carriage rides to the strut, a one-inch difference between measurements made at the leading and trailing edges of the strut represents roughly a one-degree angle-of-attack for the strut. At an angle-of-attack, the towing struts as well as the stabilizing fins shown in Figure (1) will shed tip vortices similar to those seen behind an airplane wing. At some distance downstream of the strut or fin, these shed vortices will break down into turbulence, either through flow field instability or diffusion. From this breakdown point, the turbulence decay can be treated using empirical relationships, similar to Equation (1). Brown, Reference (e) developed the following expressions relating turbulence intensity in the vortex core prior to breakdown, its radius, and the bound circulation Γ_o of a wing:

$$\frac{\sqrt{\overline{u^2}}}{V_o} = K_1 \frac{\Gamma_o / V_o}{r_c^{1/2}} \tag{5}$$

where

$$r_c = K_2 \cdot (\Gamma_o / V_o)^{2/3} \, x^{2/3} \tag{6}$$

and

$$\frac{\sqrt{\overline{u^2}}}{V_o} = \frac{K_1}{\sqrt{K_2}} \cdot \frac{(\Gamma_o/V_o)^{2/3}}{x^{1/3}} = K_3 \cdot \frac{(\Gamma_o/V_o)^{2/3}}{x^{1/3}} \tag{7}$$

where K_1, K_2 and K_3 are proportionality constants to be developed from experimental data, and Γ_o the strut or stabilizing fin root circulation. If one assumes an elliptical lift distribution for the towing strut and stabilizing fin, i.e.,

$$\frac{\Gamma_o}{V_o} = \frac{4(b/2)C_L}{\pi AR} \tag{8}$$

the wing root circulation can be related to the wing lift coefficient and geometric properties. Also, from Equation (7), it can be seen that at a fixed distance downstream of the wing, the ratio of turbulence intensity in the vortex core between two wings may be written as

$$\frac{\left(\frac{\sqrt{\overline{u^2}}}{V_o}\right)_2}{\left(\frac{\sqrt{\overline{u^2}}}{V_o}\right)_1} = \left(\frac{\Gamma_{o_2}}{\Gamma_{o_1}}\right)^{2/3} . \tag{9}$$

This result is plotted in Figure (5) and considered with Equation (8) shows the contribution of the stabilizing fins to the overall turbulence level to be much less than the contribution of the main towing strut at the same angle-of-attack. Thus for the present, we will consider only the vortices shed by the main towing strut. Experimental data, Reference (f), for a half-wing mounted on the wind tunnel floor provided the following data:

$C_L = 0.95$	$AR = 5.0$	$C = 1.00$ ft
$b/2 = 2.5$ ft	$V_o = 100$ ft/sec	$\frac{\sqrt{\overline{u^2}}}{V_o} = 0.10$ @ x=0.25 ft behind wing.

Using these data and the expressions for the turbulence levels in the vortex core prior to breakdown from Reference (g), Equations (5) through (7) become

$$\frac{\sqrt{\overline{u^2}}}{V_o} = 0.00823 \frac{\Gamma_o/V_o}{r_c^{1/2}} \tag{10}$$

$$r_c = 0.00874 \, (\Gamma_1/V_o)^{2/3} \, x^{2/3} \tag{11}$$

$$\frac{\sqrt{u^2}}{V_o} = 0.08805 \frac{(\Gamma_o/V_o)^{2/3}}{x^{1/3}} \quad . \tag{12}$$

Now, if one can estimate the time required for vortex breakdown, the turbulence levels at the breakdown point can be calculated using Equation (12). Also by assuming the turbulence intensity after the vortex breakdown is similar to Equation (1), i.e.,

$$\frac{\sqrt{u^2}}{V_o} = \frac{K}{x^{2/3}} \tag{13}$$

where K is a constant of proportionality, estimates of the turbulence level far downstream of the vortex breakdown point can be made.

Tombach, Reference (h), shows that vortex breakdown occurs at a time, t_B, between

$$\frac{15}{\varepsilon^{1/3}} \leq t_B \leq \frac{70}{\varepsilon^{1/3}} \tag{14}$$

where ε is an energy dissipation factor

$$\varepsilon = \frac{V_o^3}{\ell} \tag{15}$$

and ℓ is a characteristic length of the flow. V_c can be either the free stream velocity, V_o, as shown, or the maximum rotational velocity, V_θ, of the vortex core. Using the smaller of these two velocities, will give the largest estimate of the vortex breakdown time. For these calculations, the most appropriate length to be used in calculating the energy dissipation factor, ε, is the boundary layer displacement thickness of the body/sting combination, δ, which can be approximated using the expression for the boundary layer thickness on a flat plate, i.e.,

$$\delta = 0.37 \times \left(\frac{V_o x}{\nu}\right)^{-1/5} \tag{16}$$

and assuming a length x. Using a length x=10 ft, which makes an allowance for those portions of the body over which the flow is laminar, the vortex breakdown times can be estimated using Equations (14), (15), and (16). The various breakdown times, i.e., for the forward (data) and return carriage passes, are given in Table (2). Also, using the transformation $x_b = V_o t_B$, the distance downstream of the strut at which the vortex breaks down can be calculated. These data are also presented in Table (2). From Table (2), it can be concluded that the breakdown of the strut trailing vortex occurs almost immediately after the strut passage and that no long-standing or persistent vortices need be considered.

The lift and geometric characteristics of the DTNSRDC towing strut are given in Table (1). It was assumed that the section lift coefficient for this strut was approximately 0.10. Since an elliptical lift distribution was assumed, the section and wing lift coefficients will be equal. It was assumed that a $C_L = 0.1$ corresponded to an angle-of-attack of roughly one degree. Using the data of Table (1) and Equation (12) it is possible to calculate the turbulence level at the vortex breakdown point. Also from Equation (13), it is possible to determine the constant K. These data are also tabulated in Table (2).

Using Equation (13) it is now possible to estimate the turbulence levels arising from the strut tip vortex. For the maximum breakdown times in Table (2), the resultant turbulence levels for the strut tip vortex are given in Figure (6). Again, the increases in turbulence level occurring at 150, 350 and 550 seconds at stations Ⓒ , Ⓑ , and Ⓐ , respectively, reflect the return pass of the carriage, with the addition of the turbulence levels following Equation (4). It should also be remembered that Equation (13) holds only at times greater than the vortex breakdown time, t_B.

Other Considerations

When the velocity approaching a strut varies in the spanwise direction, a three-dimensional flow field emerges at the intersection of this strut and a wall. A vortex is shed from the intersection of the strut and the wall in a streamwise direction. Examples of this secondary flow occurs at the intersection of wings and fuselages on airplanes, and around bridge piers. From Figure (1), it can be seen that such a secondary vortex will be shed at the intersection of the strut and the 8.0-inch diameter sting supporting the model. Hawthorne, Reference (i), indicates that the incremental vortex strength is given by

$$\frac{d\Gamma}{dy} = c \frac{dv}{dy} \cdot \frac{8}{3} (th/c)^2 \{1 + \frac{4}{3} (th/c)^2\} \qquad (17)$$

for the biconvex strut used by DTNSRDC. In Equation (17), y is the spanwise independent variable and th, the maximum strut thickness. Integrating, Equation (17) becomes

$$\frac{\Gamma_o}{V_o} = \frac{8}{3} (th/c)^2 \{1 + \frac{4}{3} (th/c)^2\} \cdot c \quad . \qquad (18)$$

Again, the vortex breakdown point can be calculated using Equations (14) and (15). The appropriate length scale, Reference (g), is the momentum thickness, θ, of the strut, which can be approximated by a flat plate, i.e.,

$$\theta = 0.036c \left(\frac{V_o c}{\nu}\right)^{-1/5} \qquad (19)$$

and the appropriate velocity from $2\pi V_\theta \theta = \Gamma_o$. Following the procedure outlined in the previous section on tip vortices, the breakdown times and distances for these secondary vortices, as well as their turbulence intensity downstream from the breakdown point can be estimated using Equations (10) through (15). The breakdown times for these secondary vortices are given in Table (2). Again, it can be concluded that vortex breakdown occurs almost immediately after the strut passage, and that no long-standing or persistent vortices need be considered. For these secondary vortices, the turbulence intensities downstream from the breakdown are plotted in Figure (6) for the forward (data) pass of the carriage. Turbulence due to the secondary vortices on the return carriage pass was found to be negligible.

An estimate of the overall turbulence level from all sources, i.e., the laminar flow body drag, the towing-strut drag, the tip vortices due to a lifting strut, and the secondary vortices, is the root-mean-square total of all the components discussed or

$$\left(\frac{\sqrt{\overline{u^2}}}{V_o}\right)_{\text{Total}} = \left[\sum_{i=1}^{m} \left(\frac{\sqrt{\overline{u^2}}}{V_o}\right)_i^2\right] . \qquad (20)$$

This result is plotted as Figure (7). Here again the increases in turbulence intensity, occurring at 150, 350 and 550 seconds, reflects the return pass of the carriage.

Wake Dimensions

An estimate of the wake half-widths can be obtained rewriting Equation (2) as

$$z_{1/2} = 0.80 \frac{\sqrt{\overline{u^2}}}{V_o} \cdot x \qquad (21)$$

where x can be written as $x = V_o(t-t_o)$. For the wake half-widths only the forward (data) pass of the carriage is considered. The wake half-widths from the various sources are assumed to superimpose on each other, rather than be additive as with the turbulence intensities. Wake half-widths for the body and strut drag as well as that for the tip vortices (strut lift) are plotted for station Ⓐ in Figure (8). Only station Ⓐ is considered, since calculations for the other stations have shown that the half-widths quickly collapse to a single curve.

Conclusions

The main conclusion is drawn from Figure (7). The total carriage run, i.e., a forward and return pass, required 550 seconds. If all the turbulence sources discussed exist in a single test setup, turbulence levels would decay to less than the 0.1 percent with 1-2 minutes after the completion of a carriage run. This would be considered adequate

for the laminar flow test work. Even if the turbulence estimates were too low by a factor of two at every station, the turbulence levels would still reach an acceptable level for continued testing within 7-8 minutes after the completion of a carriage run.

Of the turbulence contributors, the drag of the towing strut appears to be the most significant. The turbulence from the laminar flow body drag and the lifting strut tip vortices are of the same order to magnitude. The turbulence generated by the secondary vortices is negligible when compared to the other turbulence sources.

References

a) Robbins, B. E., "48-Inch Water Tunnel Turbulence Level Measurements With and Without a Honeycomb," ARL Unclassified TM 77-128, April 1977.

b) Griener, L., Underwater Missle Propulsion, Compass Publications, Inc. Arlington, VA, 1967.

c) Pao, Y. H. and J. T. Lin, "Velocity and Density Measurements in the Wake of a Towed Slender Body in Stratified and Non-stratified Fluids," Flow Research Inc. Report No. 12, December 1973.

d) Chevray, R., "The Turbulent Wake of a Body-of-Revolution," ASME Transactions, Journal of Basic Engineering, pages 275-284, June 1968.

e) Brown, C. E., "Aerodynamics of Wake Vortices," AIAA Journal, Volume 11 No. 4, April 1973.

f) Arndt, R. E. A., Unpublished data, The Pennsylvania State University, 1976, University Park, PA.

g) McCormick, B. W., "A Study of the Minimum Pressure in a Trailing Vortex System," PhD Dissertation 1954, The Pennsylvania State University, University Park, PA.

h) Tombach, I., "Observations of Atmospheric Effects on Wake Vortex Behavior," AIAA Journal of Aircraft, Vol. 10 No. 11, November 1973.

i) Hawthorne, W. R., "Secondary Flows About Struts and Airfoils," Journal of the Aeronautical Sciences, September 1954.

Table No. 1: Low-Drag Body, Conventional Body, and Towing Strut Characteristics

Body Characteristics	Laminar Flow Body	Conventional Body
Overall Length, ft.	9.50	9.50
Maximum diameter, inches	25.5	25.5
Volume, ft^3	14.5	28.9
$C_{\forall}$, Prismatic Coefficient	0.432	0.86
C_D, Drag Coefficient @ 50 fps	0.012	0.060

Strut Characteristics	Strut
Chord, ft	5.0
Maximum Thickness, inches	3.75
th/c, Thickness Ratio	0.0625
Span, ft	7.0
Form	Biconvex
C_D = Drag Coefficient Based on Body Cross-section Area	0.096
C_L = For 1 Degree Angle-of-Attack, Based on Planform Area	0.10
AR = Aspect Ratio	1.40

Table No. 2 Vortex Breakdown Times and Distances, Turbulence Levels at Breakdown Point

Vortices generated by strut lift

forward (data) pass		Breakdown Time ∿ Sec	Breakdown Distance ∿ ft	$\sqrt{\overline{u^2}}/V_o$@x	K, $ft^{2/3}$
V_o = 50 ft/sec					
	minimum	0.143	7.16	0.0338	0.1256
	average	0.406	20.3	0.0239	0.1779
	maximum	0.689	33.4	0.0202	0.2095

return pass		Breakdown Time ∿ Sec	Breakdown Distance ∿ ft	$\sqrt{\overline{u^2}}/V_o$@x	K, $ft^{2/3}$
V_o = 2.5 ft/sec					
	minimum	3.50	8.75	0.0316	0.1342
	average	9.92	24.8	0.0223	0.1896
	maximum	16.333	40.8	0.0189	0.2241

Secondary Vorticity

forward (data pass)		Breakdown Time ∿ Sec	Breakdown Distance ∿ ft	$\sqrt{\overline{u^2}}/V_o$@x	K, $ft^{2/3}$
V_o = 50 ft/sec					
	minimum	0.084	4.19	0.0076	0.0199
	average	0.238	11.88	0.0054	0.0282
	maximum	0.391	19.56	0.0046	0.0332

return pass		Breakdown Time ∿ Sec	Breakdown Distance ∿ ft	$\sqrt{\overline{u^2}}/V_o$@x	K, $ft^{2/3}$
V_o = 2.5 ft/sec					
	minimum	3.73	9.32	0.0059	0.0259
	average	10.56	26.41	0.0042	0.0367
	maximum	17.40	43.5	0.0035	0.0433

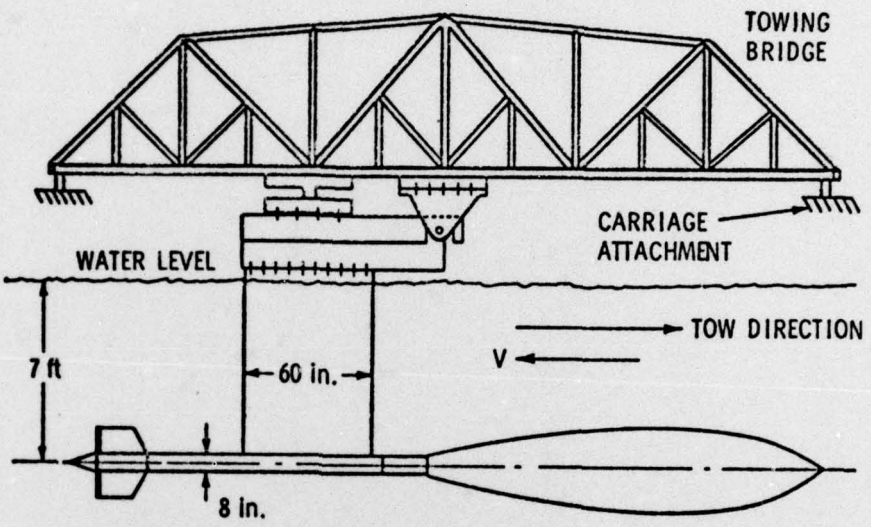

Figure No. 1: Towing Strut Geometry

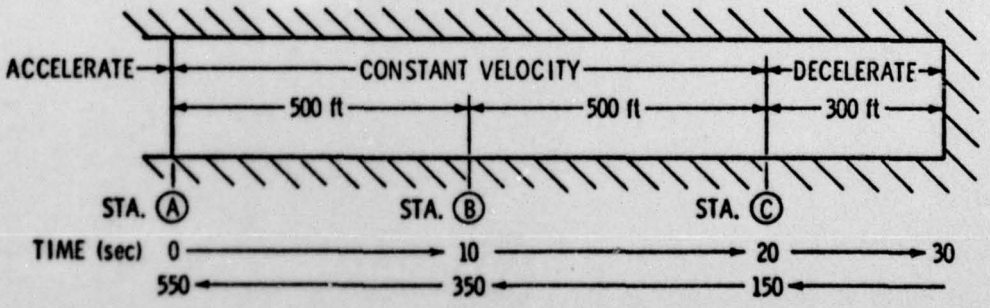

Figure No. 2: Towing Strategy and Basic Geometry

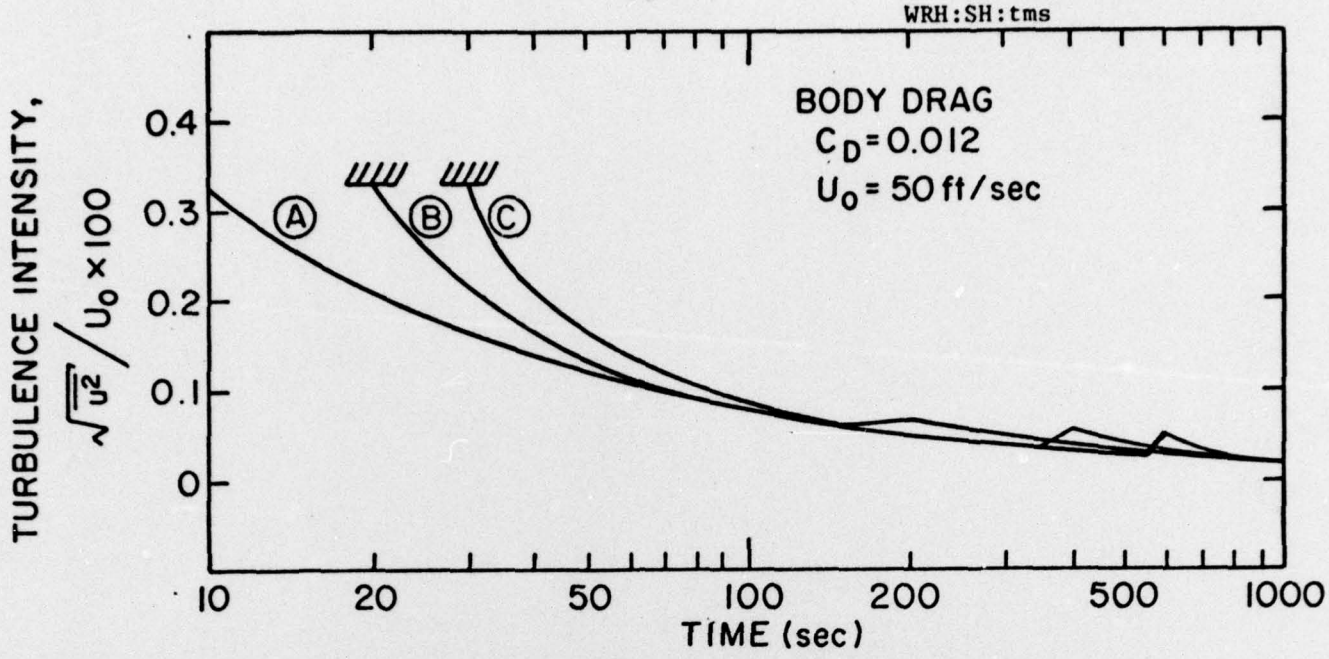

Figure No. 3: Turbulence Levels Due to Body Drag: V_o = 50 fps

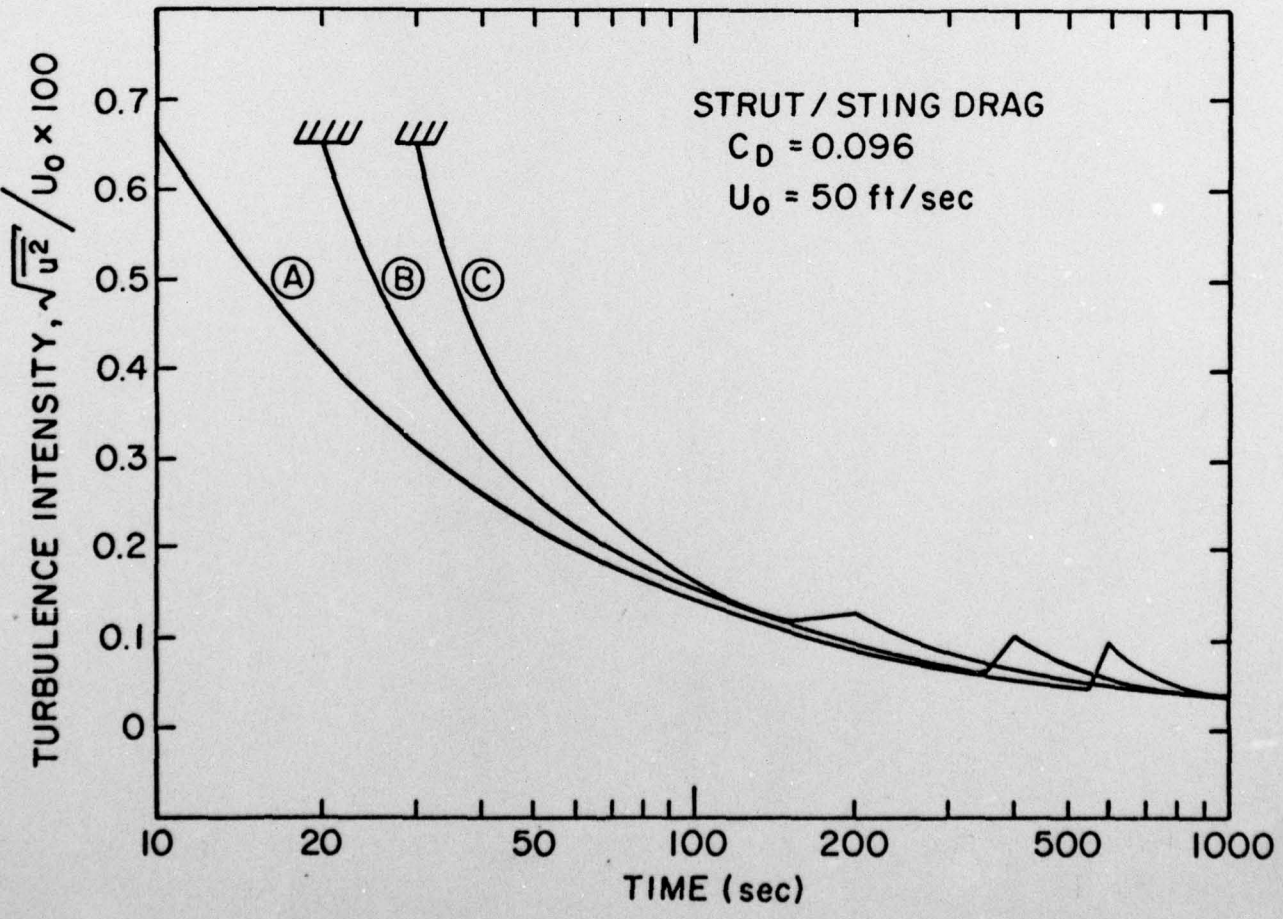

Figure No. 4: Turbulence Levels Due to Strut Drag: V_o = 50 fps

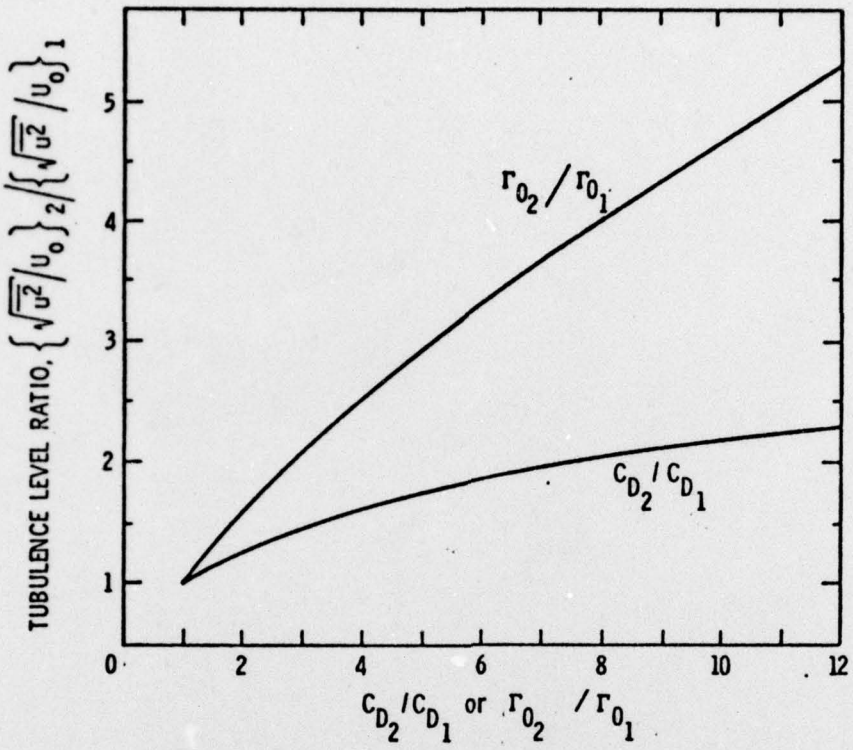

Figure No. 5: Effect of Increased System Drag or Strut Angle-of-Attack on Turbulence Levels

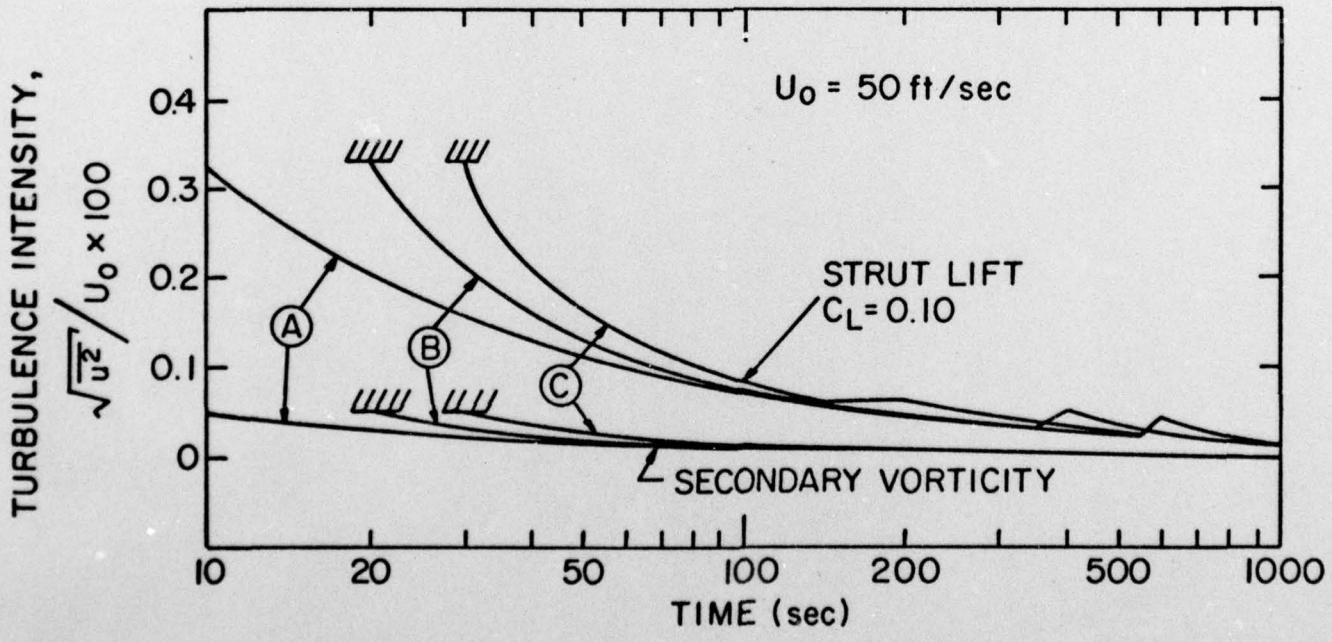

Figure No. 6: Turbulence Levels Due to Strut Lift and Secondary Vorticity: V_o = 50 fps

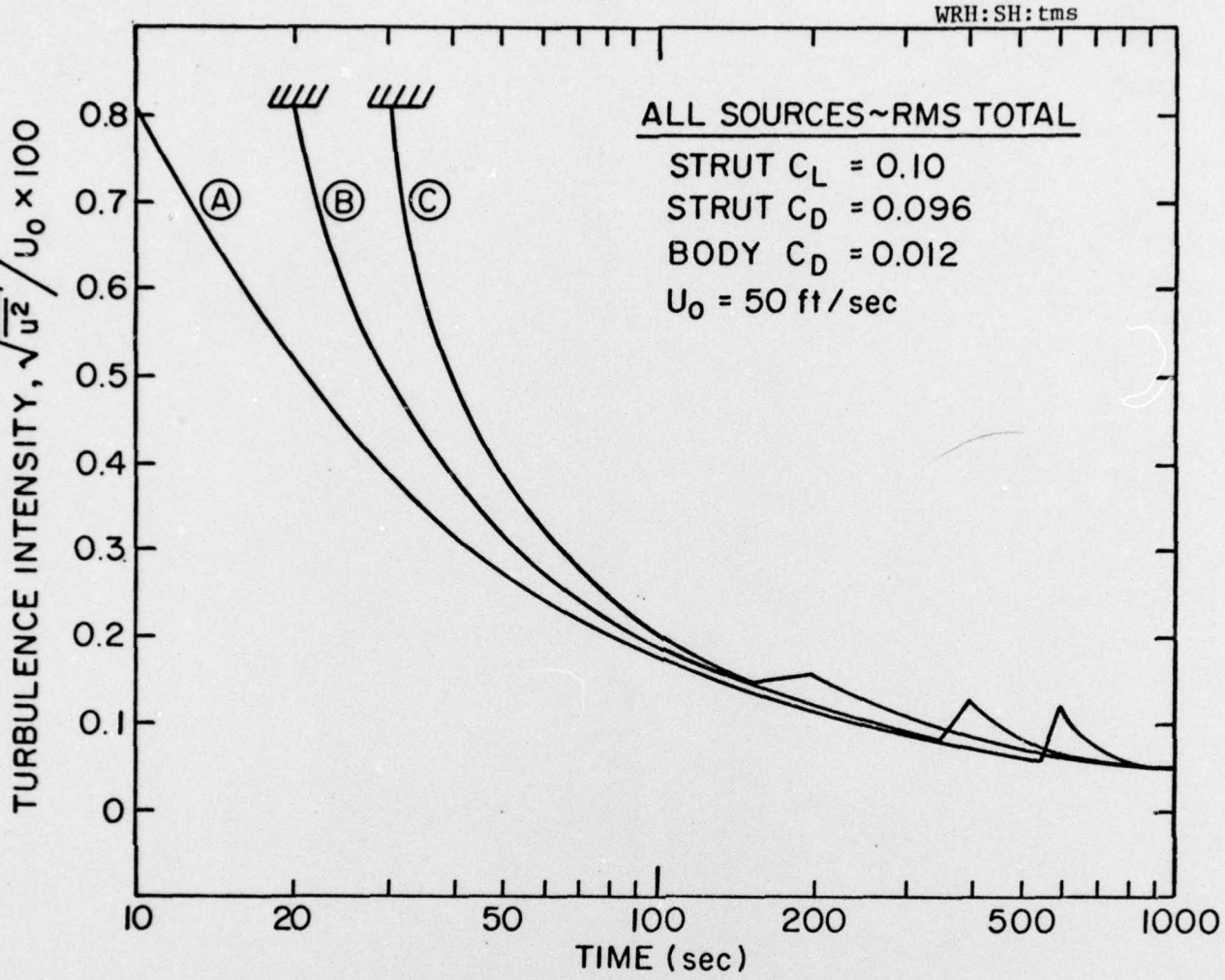

Figure No. 7: Combined Turbulence Levels From All Sources: V_o = 50 fps

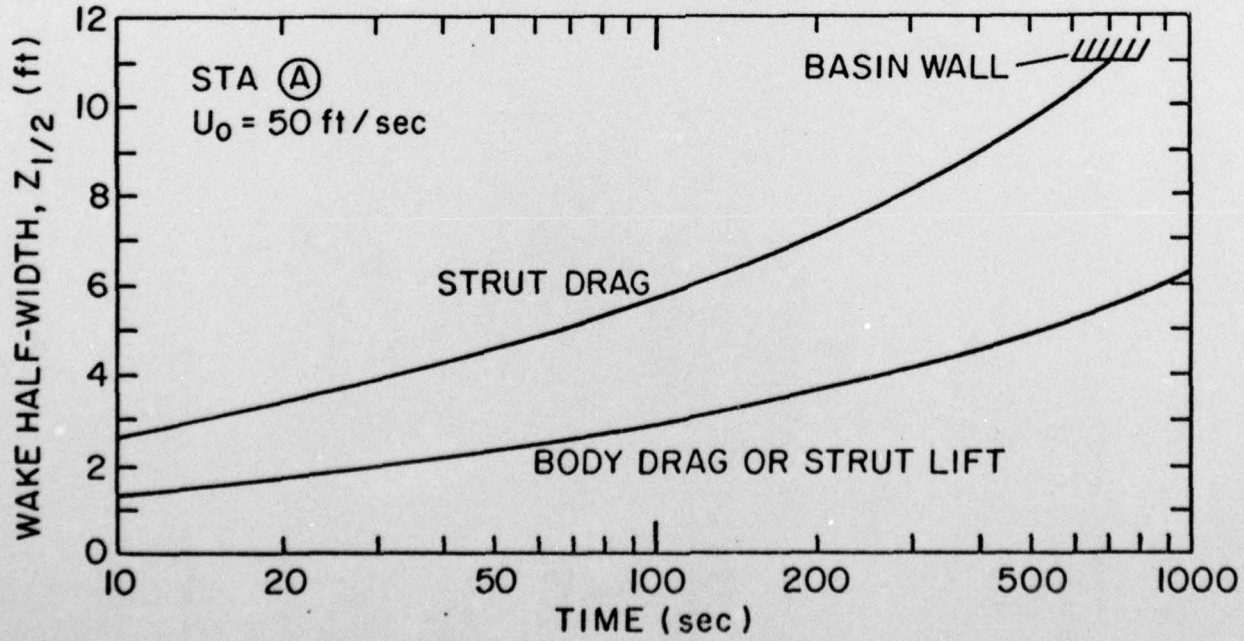

Figure No. 8: Wake Half-Widths at STA A : V_o = 50 fps

DISTRIBUTION LIST FOR UNCLASSIFIED TM 77-260 by W. R. Hall and S. Hassid, dated 19 September 1977

Commander
Naval Sea Systems Command
Department of the Navy
Washington, DC 20362
Attn: Library
Code NSEA-09G32
(Copy Nos. 1 and 2)

Naval Sea Systems Command
Attn: C. G. McGuigan
Code NSEA-03133
(Copy No. 3)

Naval Sea Systems Command
Attn: E. G. Liszka
Code NSEA-0342
(Copy No. 4)

Naval Sea Systems Command
Attn: G. Sorkin
Code NSEA-035
(Copy No. 5)

Naval Sea Systems Command
Attn: T. E. Peirce
Code NSEA-0351
(Copy No. 6)

Commanding Officer
Naval Underwater Systems Center
Newport, RI 02840
Attn: R. Nadolink
Code SB323
(Copy No. 7)

Naval Underwater Systems
Attn: R. Trainor
Code SB323
(Copy No. 8)

Naval Underwater Systems Center
Attn: F. White
Code SB332
(Copy No. 9)

Commanding Officer & Director
David W. Taylor Naval Ship R&D Center
Department of the Navy
Bethesda, MD 20084
Attn: W. E. Cummins
Code 15
(Copy No. 10)

David W. Taylor Naval Ship R&D Center
Attn: J. McCarthy
Code 1552
(Copy No. 11)

David W. Taylor Naval Ship R&D Center
Attn: W. Day
Code 1524
(Copy No. 12)

Defense Documentation Center
5010 Duke Street
Cameron Station
Alexandria, VA 22314
(Copy Nos. 13 - 24)

National Bureau of Standards
Aerodynamics Section
Washington, DC 20234
Attn: P. S. Klebanoff
(Copy No. 25)

Rand Corporation
1700 Main Street
Santa Monica, CA 90406
Attn: R. King
(Copy No. 26)

Rand Corporation
Attn: C. Gazley
(Copy No. 27)

Jet Propulsion Laboratory
Pasadena, CA 01109
Attn: L. Mack
(Copy No. 28)

DISTRIBUTION LIST FOR UNCLASSIFIED TM 77-260 by W. R. Hall and S. Hassid, dated 19 September 1977 (Continued)

Mr. W. R. Hall
APPLIED RESEARCH LABORATORY
The Pennsylvania State University
Post Office Box 30
State College, PA 16801
(Copy No. 29)

Dr. John Lumley
238 Upson Hall
Cornell University
Ithaca, NY 14852
(Copy No. 30)

Mr. S. Hassid
The Pennsylvania State University
233 Hammond Building
University Park, PA 16802
(Copy No. 31)

GTWT Library
APPLIED RESEARCH LABORATORY
The Pennsylvania State University
Post Office Box 30
State College, PA 16801
(Copy No. 32)